ASTROMETRIC REDUCTION OF PHOEBE USING A DIGITAL SHAPE MODEL. V. Viswanathan[1,2], A. J. Liounis[2], E. Mazarico[2], S. Goossens[2] and M. Neveu[2,3]; [1]University of Maryland Baltimore County, 1000 Hilltop Circ., Baltimore, MD 21250, USA; [2]NASA Goddard Space Flight Center, 8800 Greenbelt Rd., Greenbelt, MD 20771, USA (vishnu.viswanathan@nasa.gov); [3]University of Maryland, College Park, MD 20742, USA.

Introduction: The *Cassini* Imaging Science Subsystem (ISS) has provided the most spectacular images of the Saturnian system [1] and these observations constitute a fundamental dataset of high accuracy and exceptionally long-time span for the purpose of astrometry [2]. Several elaborate astrometric efforts using *Cassini* ISS data have demonstrated their use for the development and maintenance of the Saturnian satellite ephemerides and have been critical in improving our understanding of their secular orbital evolution and interior properties [3]. Astrometric efforts using images with well-resolved bodies often employ limb-based methods for center finding; this is proven to be robust for satellites with a uniform ellipsoidal shape. However, systematic biases are of concern for bodies that deviate considerably from tri-axial ellipsoids (*e.g.*, moons with irregular shapes and/or extensive features such as craters, ridges, slumps and grooves). To help understand such biases, we used the Goddard Image Analysis and Navigation Tool (GIANT) [4,5] to improve the astrometric reduction of these moons. Here we apply the method to Phoebe (Saturn IX).

Methodology: Astrometric reduction typically involves a geometric model of the camera that enables mapping of the points in the camera frame on to pixels in the images. For this study, we use the Brown camera model [6] as described below:

$$\mathbf{x}_I = \frac{1}{z_C}\begin{bmatrix} x_C \\ y_C \end{bmatrix}$$

$$r = \sqrt{x_I^2 + y_I^2}$$

$$\Delta\mathbf{x}_I = (k_1 r^2 + k_2 r^4 + k_3 r^6)\mathbf{x}_I + \begin{bmatrix} 2p_1 x_I y_I + p_2(r^2 + 2x_I^2) \\ p_1(r^2 + 2y_I^2) + 2p_2 x_I y_I \end{bmatrix}$$

$$\mathbf{x}_P = \begin{bmatrix} f_x & \alpha & p_x \\ 0 & f_y & p_y \end{bmatrix}\begin{bmatrix} (1 + a_1 T + a_2 T^2 + a_3 T^3)(\mathbf{x}_I + \Delta\mathbf{x}_I) \\ 1 \end{bmatrix}$$

where, $\mathbf{x}_I$ is a vector of image frame coordinates for the pinhole location; r is the radial distance from the principal point of the camera to the gnomic location of the point, $k_{1\text{-}3}$ are the radial distortion coefficients, $p_{1\text{-}2}$ are the tip/tilt/prism distortion coefficients, $\Delta\mathbf{x}_I$ is the distortion for point $\mathbf{x}_I$, f_x and f_y are the focal length divided by the pixel pitch in the x and y directions respectively (in px), α is a term for non-rectangular pixels, T is temperature of the camera and $a_{1\text{-}3}$ are temperature dependent coefficients and $\mathbf{x}_P$ are the pixel locations of the point in the image.

We used 117 ISS Narrow Angle Camera (NAC) images from the star cluster series in 2008 (N1580739191 to N1601342286, following [7]) to perform our own camera calibration. The observed stars in these images are matched with the GAIA EDR3 star catalog [8] to obtain their locations in the inertial frame. NAC camera model parameters such as focal length (2002.703 mm), pitch (0.012 mm/px) and image size (1024x1024 px) were used as a priori values [9]. Parameters f_x, f_y, k_1, p_1, p_2 were adjusted to minimize the residuals between the projection of the catalog-defined star locations and the positions extracted from the image. A residual attitude misalignment term per image was also included during the parameter estimation. Estimated values of the Brown camera model are provided in Table 1. Other model parameters were set to 0 as they did not show appreciable improvement to the overall star calibration residuals.

Table 1*: Brown camera model estimates for Cassini ISS's NAC using GIANT and GAIA EDR3. Uncertainties are in the last digit for estimated values.*

Parameter	Value	Equivalent value [8]	Unit
f_x	-166904.7	-166891.9	px
f_y	-166915.9	-166910.9	px
k_1	32.8		1
p_1	-0.0050		1
p_2	0.0124		1

Our estimated model is in good agreement with prior works [9] and demonstrates *Cassini* NAC's sub-pixel accuracy and minimal distortion. A residual rms of (0.059, 0.046) px was obtained after matching stars with a $M_V \leq 14$ from the Gaia EDR3 catalog. The procedure was also extended to the *Cassini* ISS Wide Angle Camera (WAC) with similar residual rms.

Data: The estimated geometric model of the cameras was then used to perform the astrometric reduction of 928 images of Phoebe between 2004 and 2007. The OPUS tool provided by the PDS Ring-Moon System Node was used for pre-selecting images based on image dimension, number of missing lines, image filter and body center resolution. Only those images with dimensions 1024x1024 px and without any missing lines were selected to avoid data processing issues. While images with clear filters (CL1 & CL2) provided the best images for astrometry, other filters were also included for this analysis. We used the cross-correlation based template matching algorithm available in GIANT for center-finding of Phoebe. A digital shape model of Phoebe [10] was used to render a template using a single-bounce ray tracer (SBRT) and a bi-directional reflectance distribution function (BRDF); a rendered template is made for each image and is cross-correlated to the ISS image for center finding.

A priori data from SPICE kernels [11] were used to reconstruct the scene in the *Cassini* NAC frame. Updated kernels from the *Cassini* Uniform Trajectory Reconstruction task were used [12]. For each image containing Phoebe, the camera's attitude was estimated using stars identified in the background. On average, 11 stars with $M_v \geq 14$ were detected per image. An example of the matching result is shown in Fig 1.

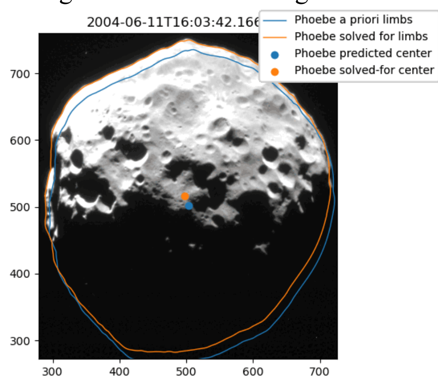

Figure 1: *Center-finding result using GIANT on an image of Phoebe (N1465662470). Observation date here is offset by the midpoint of the exposure time. Units in px.*

Results: We processed the 928 images of Phoebe from *Cassini* ISS NAC using GIANT and a shape model. The use of a high-resolution shape model for the astrometric reduction of Phoebe revealed biases of its center of figure from the *a priori* ephemerides. Overall residuals of Phoebe with respect to recent satellite ephemerides are small (and possibly negligible) for epochs without fully resolved images (see Fig 2).

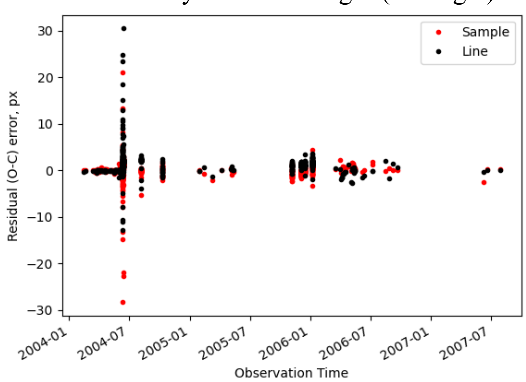

Figure 2: *Residuals of Phoebe's center of figure from Cassini ISS NAC images between 2004 and 2007.*

However, fully- and partially-resolved images of Phoebe are more sensitive to the use of simplified ellipsoidal shapes for traditional limb-fitting methods [13]. The use of Phoebe's high-resolution shape model for center-finding using GIANT helped detect biases of the order of km to tens of km on Phoebe's position with respect to Cassini's Uniform Trajectory solutions [12]. The detected biases in px were scaled by Phoebe's resolution in images (km/px) for approximate components along and orthogonal to the Sun's direction as shown in Fig. 3 (limited here to year 2004 to show clustering of residuals).

The large bias at ~80km along the positive Sun direction comes from images taken in August-2004 when the *Cassini* spacecraft was retreating from Phoebe and image resolution was poor (~36km/px).

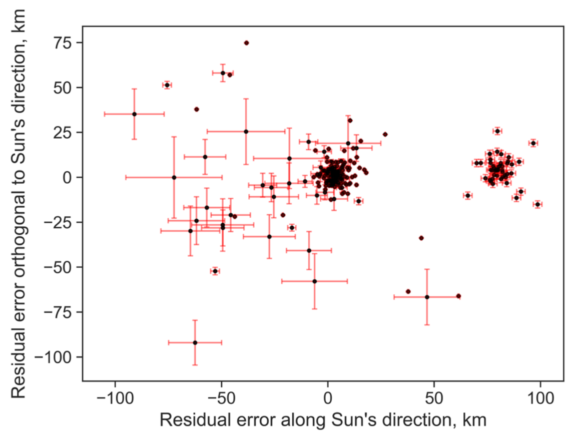

Figure 3: *Residuals of Phoebe along and orthogonal to Sun's direction obtained using GIANT. Error bars indicate uncertainties from star calibration.*

Conclusion: Astrometric reduction using high-resolution shape models enables accurate center finding and reduces biases in the center of figure of the target body; this in turn will help to improve the post-fit target trajectories. The method is particularly useful for targets with shapes deviating from a simple tri-axial ellipsoid. Future work will use the reduced images from this technique to improve Phoebe's ephemeris.

References: [1] Porco et al. (2005). *SSR*, *115*(1–4), 363–497; [2] Jacobson, R. (2018). In *42nd COSPAR* (Vol. 42, p. B5.2-37-18). [3] Lainey et al. (2017). *Icarus*, *281*, 286–296. [4] Liounis et al. (2019). In *2nd RPI Spa. Imag. Work.* (p. 14). [5] Liounis et al. (2022). GIANT Version 1.0.3, https://github.com/nasa/giant [6] Brown, D. C. (1966). *Photogram. Engg. and Rem. Sens.*, *32*(3), 444–462. [7] Tajeddine et al. (2015). *A&A*, *575*, A73. [8] Lindegren et al. (2021). *A&A*, *649*, A2. [9] Owen Jr, W. M. (2003), JPL IOM 312. *E-2003*. [10] Gaskell, R. W. (2013). *NASA PDS*, CO-SA-ISSNA-5-PHOEBESHAPE-V2.0. [11] Elson et al. (2005), CO-S/J/E/V-SPICE-6-V1.0, NASA PDS, 2005 [12] Bellerose et al. (2018) SpaceOps Conf., (AIAA 2018-2646) [13] Cooper et al. (2014). *A&A*, *572*, A43.

Acknowledgment: This material is based upon work supported by NASA under the Cassini Data Analysis Program (80NSSC21K0531).